

RESEARCH ARTICLE

10.1029/2018JD028949

Key Points:

- Effective heterogeneous ice nuclei can alter TTL cirrus microphysical properties and occurrence frequencies
- Using abundant effective IN (e.g., dust or sugar/acid organics) in TTL cirrus simulations results in disagreement with observations
- Ice nuclei can increase or decrease TTL cirrus occurrence frequency

Correspondence to:

E. J. Jensen,
eric.jensen@nasa.gov

Citation:

Jensen, E. J., Kärcher, B., Ueyama, R., Pfister, L., Bui, T. V., Diskin, G. S., et al. (2018). Heterogeneous ice nucleation in the tropical tropopause layer. *Journal of Geophysical Research: Atmospheres*, 123, 12,210–12,227. <https://doi.org/10.1029/2018JD028949>

Received 4 MAY 2018

Accepted 6 SEP 2018

Accepted article online 21 SEP 2018

Published online 8 NOV 2018

©2018. American Geophysical Union. All Rights Reserved. This article has been contributed to by US Government employees and their work is in the public domain in the USA.

Heterogeneous Ice Nucleation in the Tropical Tropopause Layer

Eric J. Jensen¹ , Bernd Kärcher² , Rei Ueyama¹ , Leonhard Pfister¹ , Theopaul V. Bui¹ , Glenn S. Diskin³ , Joshua P. DiGangi³ , Sarah Woods⁴ , R. Paul Lawson⁴ , Karl D. Froyd⁵ , and Daniel M. Murphy⁶ 

¹NASA Ames Research Center, Moffett Field, CA, USA, ²Deutsches Zentrum für Luft- und Raumfahrt, Oberpfaffenhofen, Germany, ³NASA Langley Research Center, Hampton, VA, USA, ⁴Spec, Inc., Boulder, CO, USA, ⁵NOAA Earth System Research Laboratory and Cooperative Institute for Research in Environmental Science, Boulder, CO, USA, ⁶Chemical Sciences Division, NOAA Earth System Research Laboratory, Boulder, CO, USA

Abstract Recent laboratory experiments have advanced our understanding of heterogeneous ice nucleation at low temperatures. We use these laboratory results, along with field measurements of aerosol composition, to constrain a parameterization of heterogeneous nucleation rate dependence on temperature and supersaturation. We apply this nucleation parameterization in detailed simulations of transport and cloud formation in the Tropical Tropopause Layer (TTL, $\approx 14\text{--}18$ km) constrained by high-altitude aircraft measurements of TTL cirrus microphysical properties and supersaturation. The model results indicate that if the abundant TTL organic-containing aerosols were effective glassy ice nuclei (IN), as indicated by laboratory experiments with simple sugars/acids, then heterogeneous nucleation would prevent the occurrences of large ice concentrations and large ice supersaturations, both of which are clearly indicated by the in situ observations. If glassy organic aerosols are relatively poor IN, as indicated by laboratory experiments with more atmospherically relevant secondary organic aerosol-like composition, then the simulated ice concentrations and supersaturations are in reasonable agreement with the observations. Concentrations of effective mineral dust or ammonium sulfate IN larger than about 50/L can drive significant changes in cirrus microphysical properties and occurrence frequency. The cloud occurrence frequency can either increase or decrease, depending on the efficacy and abundance of IN added to the TTL. Relatively low TTL concentrations of mineral dust particles ($\leq 10\text{ L}^{-1}$ indicated by the limited available field measurements) have negligible impact on cirrus frequencies or microphysical properties. Given the assortment of uncertainties, meaningful estimates of TTL aerosol-cirrus indirect effects on radiative forcing are likely not possible at this time.

1. Introduction

The initial stage of upper tropospheric cirrus cloud formation involves nucleation of ice crystals, and the details of the ice nucleation process can affect the subsequent development and microphysical properties of the clouds. A large number of laboratory experiments, field experiments, and modeling studies have been focused on understanding ice nucleation processes. Homogeneous freezing of aqueous aerosols is known to occur in some cases when rapid cooling drives nucleation of numerous ice crystals (Jensen et al., 1998, 2013), and this process is relatively well understood and well represented in models since the homogeneous freezing nucleation rate is essentially independent of the detailed aerosol composition (Koop et al., 2000). In contrast, heterogeneous nucleation on solid particles (either deposition nucleation on dry particles or immersion freezing on insoluble inclusions in mixed-phase aerosols) is much more complicated with marked dependencies on particle composition, surface morphology, and phase. The balance between heterogeneous and homogeneous nucleation has implications for cirrus microphysical properties and radiative forcing (Gettelman et al., 2015; Lohmann et al., 2004). Heterogeneous ice nuclei (IN) are likely changing in response to anthropogenic activities (Cziczo et al., 2009; Kärcher, 2017; Neff et al., 2008). In addition, modification of cirrus lifetimes and radiative properties by injection of IN into the upper troposphere is one of the proposed *geoengineering* methods for offsetting the surface-warming effects of increasing greenhouse gases (Gasparini & Lohmann, 2016; Lohmann & Gasparini, 2017; Mitchell & Finnegan, 2009; Penner et al., 2015; Storelvmo et al., 2013).

A number of recent laboratory experiments have provided new information about the physical properties of aerosols at low temperatures and their ability to act as ice nuclei. In particular, experiments have revealed that organic-containing aerosols transition to a highly viscous glassy state at low temperatures relevant for the upper troposphere (Murray, 2008; Price et al., 2015; Zobrist, Marcolli, Pedernera, et al., 2008). As shown by Wilson et al. (2012) and others, the glass transition temperature depends on the detailed composition of the organic aerosols. Further experiments have shown that these glassy particles are moderately effective as ice nuclei (Murray et al., 2010; Wilson et al., 2012), although the threshold supersaturation for activation of glassy IN depends on the types of organics in the aerosols (Schill et al., 2014; Wagner et al., 2017). In addition, a number of experiments have constrained the effectiveness of mineral dust as ice nuclei at low temperatures (e.g., Ullrich et al., 2017), and solid ammonium sulfate has been shown to be an effective ice nucleus (Abbatt et al., 2006). These experimental results (particularly for glassy, organic-containing aerosols) are especially relevant for formation of cirrus clouds in the cold uppermost tropical troposphere where temperatures below 200 K prevail.

We focus here on the tropical tropopause layer (TTL, 14–18 km). Optically thin cirrus are ubiquitous in the TTL (Wang et al., 1996), and they regulate the abundance of water vapor entering the stratosphere, which in turn has important climate impacts (Forster & Shine, 2002; Solomon et al., 2010). Radiative heating in TTL cirrus also contributes significantly to the local thermal budget (Yang et al., 2010). The upper TTL represents a unique dynamical environment, with slow ascent, stronger thermal stability than the middle troposphere, and relatively infrequent influence from deep convection. The upper TTL ascent is essentially an extension of the stratospheric Brewer-Dobson circulation driven by wave breaking. In balance with this ascent, the upper TTL is radiatively heating, and optically thin cirrus play an important role in the thermodynamic balance. Radiative transfer calculations including cloud effects indicate that the crossover between radiative cooling (large-scale descent) below and radiative heating (ascent) above occurs at about 15 km (Yang et al., 2010). We refer to this height as the level of zero radiative heating. Note that this crossover level varies between about 13 and 16 km across the tropics, depending primarily on the vertical distribution and optical properties of tropospheric and TTL clouds.

As shown below, air parcels typically undergo multiple in situ cirrus formation events on their approximately 1-month journey upward through the TTL. Therefore, even if a source such as deep convection supplies ice nuclei to the lower-middle TTL, there is a potential for removal of these IN when they nucleate ice crystals that subsequently fall out of the rising air parcels. This nucleation-scavenging process may effectively deplete IN such that cirrus formation near the cold-point tropopause (the final dehydration events before entry into the stratosphere) is dominated by homogeneous freezing, with implications for the abundance of water vapor entering the stratosphere. The impacts of IN on TTL cirrus microphysical properties (ice crystal concentration and size) may also depend on the IN scavenging process. The impact of heterogeneous nuclei on TTL cirrus has been examined previously using parcel-model simulations (Barahona & Nenes, 2011; Kärcher, 2004; Spichtinger & Krämer, 2013) and by our group with one-dimensional simulations and simple threshold specification of ice nuclei (Jensen et al., 2016). Here we use the same modeling framework as in our previous study (one-dimensional simulations along trajectories with high-frequency wave temperature perturbations superimposed), but we include heterogeneous nuclei temperature and supersaturation dependence based on the laboratory experiments, and we constrain the abundance of different IN types with field measurements.

In this study, we first review the recent laboratory experiments quantifying ice nucleation rates for glassy organic-containing aerosols, mineral dust, and ammonium sulfate aerosols at low temperatures (section 2). Field measurements of TTL aerosol and cirrus physical properties are described in section 3. Next, we develop a generalized framework for specifying nucleation properties of ice nuclei at low temperatures in numerical models, and we determine parameter values appropriate for glassy aerosols and mineral dust based on the laboratory experiments (section 4). We implement the IN parameterization in a detailed one-dimensional model of TTL transport and cirrus formation (section 5). The individual IN is tracked, and the sedimentation and scavenging processes are included. With different assumptions about the initial IN abundance, we evaluate the impact of IN on TTL cirrus occurrence frequencies, cirrus microphysical properties, and the occurrence of supersaturation with respect to ice (section 6). The model results are constrained by statistical comparisons with high-altitude aircraft measurements of TTL ice cloud microphysical properties and supersaturation. A summary of the results and a discussion of the implications are provided in section 7.

2. Recent Laboratory Measurements of Low-Temperature Aerosol Properties and Ice Nucleation

Recent laboratory research has advanced our understanding of the physical state and ice nucleation efficiency of atmospherically relevant aerosol types at low temperatures. It is now well established that organic-containing aerosols transition to a highly viscous glassy state at low temperatures (Koop et al., 2011; Murray, 2008; Zobrist, Marcolli, Pedernera, et al., 2008), potentially preventing homogeneous freezing of the aerosols. Further work showed that glassy aerosols can act as heterogeneous ice nuclei at low temperatures (Murray et al., 2010; Wilson et al., 2012). These studies showed that small fractions (as high as about 0.004 during the cloud chamber expansion experiments) of the glassy aerosols can act as heterogeneous nuclei at TTL temperatures when the ice saturation ratio (S_i) exceeds about 1.2–1.4. The fractions of organic aerosols acting as heterogeneous ice nuclei vary widely depending on the detailed organic composition of the particles (Wilson et al., 2012). Experiments using simple sugars/acids (Baustian et al., 2013; Murray et al., 2010; Wilson et al., 2012) indicated relatively low supersaturation threshold for ice nucleation on a fraction of the glassy aerosols. Other ice nucleation experiments used aerosol compositions that were better proxies for atmospheric secondary organic aerosols (SOA) such as α -pinene (Ignatius et al., 2016; Ladino et al., 2014; Möhler et al., 2008; Prenni et al., 2009; Wang et al., 2012; Wagner et al., 2017). The supersaturation thresholds for ice nucleation on the SOA particles were considerably higher, and in some cases ice nucleation did not occur until the supersaturation exceeded the threshold for homogeneous freezing of aqueous aerosols ($S_i \approx 1.6$ at TTL temperatures). Relatively little is known about the detailed composition of TTL aerosols, but the available measurements indicate that most TTL aerosols contain significant mass fractions of oxidized organics (see discussion of TTL aerosol composition measurements below).

Wagner et al. (2012) found that homogeneous freezing of organic-containing aerosols at temperatures above the glass transition, followed by sublimation of the ice, can leave behind preactivated glassy aerosols with very low thresholds for subsequent heterogeneous ice nucleation. For most of the organic aerosol compositions tested in the laboratory, aerosols would already be in the glassy state before ice nucleation occurs at TTL temperatures ($T < 205$ K; Wilson et al., 2012), in which case this preactivation pathway would typically not occur. Wagner et al. (2017) recently showed that liquid/ice cloud processing of α -pinene aerosols in a laboratory-simulated convective-updraft environment increases the effectiveness of the particles as IN considerably. The origin of TTL aerosols is presumably either new-particle formation in the upper troposphere (Brock et al., 1995) or transport by deep convection (Froyd et al., 2009). In the latter case, ice nuclei presumably participated in nucleation of ice crystals in the convective updrafts and were released after sublimation of ice crystals in short-lived convectively generated cirrus, potentially implying that the aerosols were preactivated.

Berkemeier et al. (2014) used a semiempirical model of organic aerosol physical state transformations to show that for typical updraft speeds, glass/liquid core shell morphologies can persist, allowing immersion freezing nucleation to occur. Lienhard et al. (2015) further showed that transitions to the glass state may not be complete, such that aqueous aerosol surface layers remain, permitting homogeneous freezing. Schill et al. (2014) showed that glassy SOA particles generated by aqueous chemical processing were poor IN in the deposition mode. However, if ammonium sulfate were present in the aerosols, amorphous deliquescence of the aqueous SOA could occur, and the crystalline ammonium sulfate could serve as an immersion IN allowing ice nucleation at lower supersaturation than that required for deposition nucleation (Schill & Tolbert, 2013). The laboratory results suggest that the mixed-phase state of organic aerosols may primarily occur at warmer temperatures than encountered in the TTL; that is, at TTL temperatures, most organic-containing aerosols are likely fully glassy such that deposition nucleation is the only available ice-formation pathway. Wang et al. (2012) showed that glassy SOA particles act as deposition IN at temperatures between 200 and 230 K, whereas partial amorphous deliquescence permits immersion freezing at warmer temperatures.

The leading particle type acting as heterogeneous ice nuclei in the midlatitude upper troposphere is mineral dust (e.g., Chen et al., 1998; Cziczo & Froyd, 2014), and numerous laboratory experiments have examined the efficiency of various types of mineral dust as IN (see Hoose & Möhler, 2012, and references therein). The effectiveness of dust IN can depend on the detailed morphology of the particles and the presence of liquid coatings on the aerosols. Zobrist, Marcolli, Peter, et al. (2008) showed that the threshold for immersion freezing of solution-coated dust particles primarily depends on the solution water activity (similar to homogeneous freezing of aqueous aerosols).

Another candidate for ice nuclei in the TTL is crystalline ammonium sulfate. Laboratory experiments have shown that effloresced ammonium sulfate particles can be effective ice nuclei (Abbatt et al., 2006; Baustian et al., 2009; Wise et al., 2009), and given the low TTL temperatures, the relative humidity with respect to liquid water along parcel trajectories typically drops below the efflorescence relative humidity (ERH) of ammonium sulfate (Jensen et al., 2010). As discussed below, measurements of TTL aerosol composition generally indicate that the aerosol sulfate is either partially or fully neutralized (Froyd et al., 2009). Bodsworth et al. (2010) found that the addition of organics to sulfate particles reduces the ERH of ammonium sulfate at upper tropospheric temperatures, possibly preventing efflorescence in TTL aerosols. It is unclear whether efflorescence of ammonium sulfate typically occurs in TTL aerosols, but if crystalline ammonium sulfate is present, it could permit immersion freezing of internally mixed inorganic/organic aerosols at lower supersaturations than those required for deposition nucleation on SOA-like glassy aerosols (Schill & Tolbert, 2013; Schill et al., 2014).

3. Field Measurements in the Tropical Tropopause Layer

3.1. Aerosol Measurements

Relatively little is known about the actual composition and physical state of aerosols in the tropical tropopause layer. What direct information we do have comes primarily from the single-particle mass spectrometer (PALMS) flown on a high-altitude aircraft (Froyd et al., 2009). The PALMS instrument ionizes particles larger than about 0.2 μm diameter and uses a mass spectrometer to identify the ion fragments, providing semi-quantitative information about aerosol composition. The PALMS measurements in the TTL near Costa Rica during Boreal wintertime indicated that the great majority of particles sampled contained sulfates and oxidized organics, with average organic mass fractions as high as 80% in the lower TTL and decreasing to about 30–40% near the tropopause. Mineral dust concentrations were depleted in the TTL relative to measurements in lower free-tropospheric regions (TTL dust concentrations less than about 10 L^{-1} , Froyd et al., 2009, $1 \text{ cm}^{-3} = 1,000/\text{L}$, whereas dust concentrations at lower free tropospheric altitudes are typically several tens per liter or higher), perhaps indicating that transport of dust into the TTL is inefficient or dust particles are scavenged from the TTL by ice nucleation followed by sedimentation. Ammonium sulfate was commonly present in the TTL aerosols sampled, but it was generally internally mixed with organics. At altitudes extending into stratospheric air masses, sulfuric acid particles dominated, and some of the particles contained meteoric material.

During the 2006 Costa Rica Aura Validation Experiment (CR-AVE), PALMS was flown with a counterflow virtual impactor inlet that allowed measurements of the composition of residual particles left behind after ice crystals sublimated. Note that these measurements were limited to ice crystal sizes smaller than about 30–50 μm (Cziczo & Froyd, 2014). However, very few TTL cirrus ice crystals grow to sizes larger than 50 μm (Lawson et al., 2008). Since aerosol impaction scavenging by falling ice crystals is likely negligible for the small ice crystals typically present in the TTL, the residual particles probably served as ice nuclei. Froyd et al. (2010) reported that the cirrus residual particle compositions were generally not markedly different than the compositions of ambient TTL aerosols outside the cirrus. Neither mineral dust nor meteoric material were enhanced in the cirrus residual particles. These findings could suggest that homogeneous freezing of aqueous internally mixed particles was the dominant ice nucleation process. Alternatively, the predominantly internally mixed sulfate organic particles could have been in a glassy state and served as heterogeneous ice nuclei. It is also possible that crystalline ammonium sulfate in the particles promoted heterogeneous ice nucleation.

As noted above, PALMS does not provide information about aerosol composition for sizes smaller than 0.2 μm . Smaller, *nucleation-mode* aerosols can be quite abundant in the TTL (Brock et al., 1995; Weigel et al., 2011), although they may be too small to serve as effective IN (DeMott et al., 2010). The composition of these ultrafine aerosols likely depends on the time since the most recent new-particle formation event. Presumably, over time, organics will condense on the ultrafine aerosols.

Based on the available laboratory and field information, we suggest that glassy organic-containing aerosols, mineral dust, and mixed-phase aerosols with crystalline ammonium sulfate are all viable candidates for TTL ice nuclei. Field measurements in the upper troposphere are increasingly indicating that aerosols commonly include substantial organic mass fractions, and multiple laboratory experiments indicate that these aerosols should be glassy under the very cold TTL conditions. The PALMS measurements also indicate that TTL aerosol sulfate is typically neutralized, and if efflorescence occurs, the crystalline ammonium sulfate could serve as an effective immersion-freezing IN (Schill et al., 2014). The available field evidence suggests relatively low concentrations of mineral dust (Froyd et al., 2009), but these measurements were made in a single location

and season, far downstream of deep convection sources, and they may not be representative of TTL dust abundance in general.

3.2. Cirrus Microphysics and Relative Humidity Measurements

The simulations of TTL cirrus cloud properties discussed below are constrained with recent high-altitude aircraft measurements of ice crystals and ice supersaturation. The Airborne Tropical Tropopause Experiment (ATTREX; Jensen et al., 2017) and the Pacific Oxidants, Sulfur, Ice, Dehydration, and cONvection experiment (POSIDON) each provided extensive measurements of TTL cirrus and relative humidity. Size distributions of TTL cirrus ice crystals were measured with the Fast Cloud Droplet Probe (FCDP; McFarquhar et al., 2007) and the two-dimensional stereo probe (2D-S; Lawson et al., 2006). The FCDP measures the forward scattered laser light from individual cloud particles with sizes ranging from 1- to 50- μm diameter, whereas the 2D-S probe captures images of ice crystals with size ranging from 10 μm to 4 mm. Ice number concentration will be the primary measure of TTL cirrus properties used for comparison with simulations. Since ice crystals smaller than 10 μm can be abundant in TTL cirrus (Jensen et al., 2013), we focus here on the FCDP ice concentrations. Given the FCDP sample volume of 0.08 L/s (Thornberry et al., 2017), the minimum detectable ice concentration in 1-s samples is about 15 L⁻¹. We note also that the vast majority of ATTREX and POSIDON measurements were made well away from deep convection systems, and the ice concentration data sets should therefore be overwhelmingly dominated by cirrus formed in situ in the TTL.

Past aircraft measurements of cirrus microphysical properties have suffered from artifacts caused by shattering of large ice crystals on impaction with instrument inlets or probe tips (e.g., Field et al., 2006; Jensen et al., 2009; McFarquhar et al., 2007). The TTL cirrus measurements presented here should not be significantly affected by shattering artifacts for two reasons: First, postprocessing analysis of particle interarrival times is used to identify and remove clusters of particles caused by crystal shattering (Baker et al., 2009; Lawson, 2011). Second, in TTL cirrus clouds, ice crystals large enough to shatter (maximum dimensions larger than 100 μm) are exceedingly rare (Lawson et al., 2008).

The statistics of supersaturation with respect to ice are derived from ATTREX and POSIDON measurements of water vapor concentration, pressure, and temperature. We use the Diode Laser Hygrometer (DLH) water vapor measurements that have excellent precision at 1-Hz time resolution. The internal-path tunable-diode laser NOAA Water (NW) instrument (Thornberry et al., 2015) was also included in the ATTREX and POSIDON payloads, and the agreement between the DLH and NW water vapor measurements was excellent (Jensen et al., 2017). We use temperature and pressure measurements from the Meteorological Measurement System (MMS). Given the 5% DLH H₂O concentration uncertainty and 0.3 K MMS temperature uncertainty, the RHI uncertainty is no more than 10–15%. As shown by (Jensen et al., 2017), the in-cloud relative humidity distribution is centered exactly on 100%, which strongly suggests there is no significant systematic error in the relative humidity measured during ATTREX. Imperfect precision of the measurements will broaden the RHI frequency distribution. Using the estimated DLH H₂O and MMS temperature precisions of 50 ppbv and 0.05 K, respectively, we estimate that the broadening of the ice saturation ratio frequency distribution at an $S_i = 1.4$ would be no greater than 0.03, which is negligible compared to the differences between simulated S_i distributions shown below.

4. Model Representation of TTL Ice Nuclei

4.1. Parameterization for Heterogeneous Ice Nucleation at Low Temperatures

Since no parameterization currently exists specifically for heterogeneous ice nucleation at cold TTL temperatures, we have developed the following framework. The heterogeneous nucleation rate coefficient (J , in units of cm⁻² s⁻¹) may depend explicitly on air temperature, T , and ice supersaturation, $S_i(T)$. Small relative changes of J are given by a Taylor expansion:

$$d \ln J = \underbrace{\frac{\partial \ln J}{\partial S_i} \Big|_T}_{\alpha} dS_i + \underbrace{\frac{\partial \ln J}{\partial T} \Big|_{S_i}}_{-\lambda} dT, \quad (1)$$

allowing us to express $J(S_i, T)$ in the form

$$\ln J = \alpha(S_i - S_o) - \lambda(T - T_o) + \ln J_o, \quad (2)$$

where the constant $J_o \equiv J(S_o, T_o)$ represents the nucleation efficiency of a particular type of insoluble ice nuclei (IN), that is, J_o represents conditions where ice formation is significant on atmospherically relevant time

scales. Equation (2) holds for small variations of S_i and T around threshold values $\{S_o, T_o\}$. Away from those thresholds, the accuracy of the J representation does not matter, since either very few ice crystals have formed or the freezing event has already terminated. In general equation (2) is applicable to either deposition or immersion nucleation.

We may estimate α by comparison with the water activity approach for homogeneous freezing (Koop et al., 2000), in which case this coefficient is given by $\alpha_{\text{hom}} = (\partial \ln J_{\text{hom}} / \partial S_i)|_T$, where $J_{\text{hom}}(a_w, T)$ is the homogeneous freezing rate coefficient and $a_w(T)$ is the water activity in aqueous solutions. Assuming that aerosol particles remain in equilibrium with the vapor during cooling ($a_w = S_w$), da_w can be related to dS_i at constant T via $da_w = dS_w = dS_i p_{\text{sat},i} / p_{\text{sat},i}$ and the Clausius-Clapeyron equation. With this equilibrium assumption, equation (2) resembles earlier parameterizations for immersion freezing based on water activity (Kärcher & Lohmann, 2003; Knopf & Alpert, 2013); α_{hom} yields the steepest possible dependence of J on ice supersaturation (or water activity), because homogeneous freezing occurs over a very narrow range of S_i (a_w) and the dependence is likely to be flatter for heterogeneous nucleation.

For comparison with laboratory measurements, we define the fraction of aerosol particles containing IN that nucleate to form ice crystals in a time span δt (e.g., Herbert et al., 2014) as

$$f_{\text{ice}} = 1 - \exp(-JA\delta t), \quad (3)$$

where A is the IN surface area. This formulation allows superposition of a variety of IN with different values for the set of parameters $\{S_o, T_o, J_o, \alpha, \lambda\}$.

4.2. Application of Active Site Density Specification

Another commonly used approach to quantification of IN activity is specification of the ice nucleation active site (INAS) density (DeMott, 1995). This approach is deterministic in that the density of active sites is specified as a function of temperature and ice saturation ratio, and no time dependence is included. The active site density is related to the fraction of aerosols active as ice nuclei by

$$f_{\text{ice}} = 1 - \exp(-An_s) \quad (4)$$

where n_s is the surface density of active sites on a particle with surface area A .

Since the sample exposure times for the nucleation experiments is generally not provided, it is not straightforward to determine a nucleation rate (required for the stochastic approach) from the active site density expressions. Rather, we assume that the number of new ice crystals nucleated in a model time step is determined by the active site density for the new temperature and saturation ratio as well as the available IN concentration

$$\Delta N_{\text{ice}} = N_{\text{IN}} (1 - \exp^{-An_s(T,S_i)}) \quad (5)$$

The activated ice nuclei are depleted from the available IN population. Since we use very small time steps (seconds) during nucleation events, the competition between supersaturation depletion by existing ice crystals and supersaturation increase by cooling is properly treated. This competition can control the number of ice crystals nucleated when large concentrations of IN are available, as in homogeneous freezing events.

4.3. Specification of TTL Ice Nuclei Properties

As discussed above, recent laboratory experiments have helped to quantify the effectiveness of various particle types as ice nuclei. Most of the ice nucleation experiments only provide the threshold supersaturation where ice formation is first observed on the sample particles. These threshold supersaturations correspond to small fractions of the sample particles promoting ice nucleation. The cloud chamber nucleation experiment results are reported as fractions of aerosols frozen versus supersaturation in some cases (e.g., Murray et al., 2010; Wilson et al., 2012). Many of the deposition nucleation results are also quantified by specifying the surface density of active sites that promote ice nucleation (see discussion below).

The reported frozen fractions from the cloud chamber experiments are actually cumulative fractions of aerosols promoting ice nucleation measured in cooling experiments. For specification of our heterogeneous nucleation model parameters, we calculate the frozen fraction versus time in a cooling parcel with a cooling rate approximately equal to that used in the AIDA cloud chamber experiments (≈ 1 K/min (Wilson et al., 2012)).

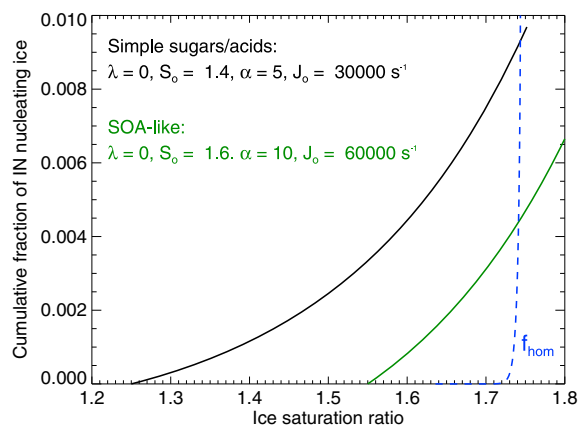


Figure 1. The cumulative fractions of glassy aerosols frozen versus ice saturation in an air parcel cooling from an initial temperature of 196 K are shown. We have used parameters in our nucleation model that give approximate agreement with the laboratory experiments using organic aerosols composed of simple sugars/acids (black curve) and more atmospherically relevant SOA proxies (green curve). Also shown is the fraction of aqueous aerosols that freeze homogeneously at a temperature of 188 K with a cooling rate of 1 K/min (blue dashed curve).

At TTL temperatures, the threshold ice saturation ratios for onset of ice nucleation on glassy aerosols composed of simple sugars/acids are typically about 1.3–1.4 at TTL temperatures (<205 K) (Baustian et al., 2013; Murray et al., 2010; Wilson et al., 2012). To represent these experiments, we use an S_0 value of 1.4. Since no information about temperature dependence is available from these experiments, we assume $\lambda = 0$ (no explicit temperature dependence). We find that using $\alpha = 5$ and $J_0 = 30,000 \text{ cm}^{-2} \cdot \text{s}^{-1}$ give a buildup of f_{ice} in approximate agreement with the supersaturation dependence shown by Wilson et al. (2012). As discussed above, the experiments with SOA-like aerosols generally indicate ice nucleation onset at supersaturations just below the threshold for homogeneous freezing. We represent the SOA-like experiments with $S_0 = 1.6$, $\alpha = 10$, and $J_0 = 60,000 \text{ cm}^{-2} \cdot \text{s}^{-1}$. The cumulative frozen fractions calculated with these sets of parameters are shown in Figure 1.

As discussed above, numerous laboratory experiments have examined the ice nucleating efficiency of various types of mineral dust. Ullrich et al. (2017) provided a parameterization based on a number of these experiments using the deterministic INAS approach. Ullrich et al. (2017) provided a fit to the measured active site density versus ice saturation ratio and temperature. Here we use modified parameters in their active site density expression (equation (7) in Ullrich et al., 2017) that are more appropriate for the low temperatures encountered in the TTL. Assuming a particle size

of $0.3 \mu\text{m}$, we use equation (4) to calculate the corresponding fractions frozen versus saturation ratio and temperature (Figure 2). Note that dust ice nucleation efficiency decreases sharply with decreasing temperature below about 200 K (Figure 2), indicating that dust particles are relatively poor ice nuclei at the coldest temperatures occurring near the tropical tropopause.

The laboratory experiments indicate that dust particles are much more efficient as ice nuclei than glassy organic aerosols: frozen fractions approach unity at high supersaturation for dust, whereas the reported frozen fractions for glassy aerosols are no larger than about 0.01 at supersaturations below the homogeneous freezing threshold. However, as discussed above, the PALMS measurements indicate relatively low concentrations of mineral dust in the TTL (about $5\text{--}10 \text{ L}^{-1}$), although concentrations could be considerably higher closer to mineral dust source regions and deep convection. In contrast, the PALMS measurements show that most of the sampled TTL aerosols (larger than $0.2 \mu\text{m}$ diameter) have substantial organic mass fractions, and the laboratory experiments indicate that such aerosols will likely be glassy at TTL temperatures, resulting in a potentially large population of glassy aerosols available as IN.

Measurements indicate that the TTL aerosol concentration (including ultrafine particles) is typically around 300 cm^{-3} , with a great deal of variability associated with proximity to new particle formation events (Weigel et al., 2011). The accumulation-mode aerosol concentration is typically about 20 cm^{-3} (Froyd et al., 2009). We have no information about the composition of ultrafine particles, but if their composition is similar to the accumulation-mode compositions indicated by the PALMS measurements, and if we assume that on the order of half of them are in a glassy state, the resulting concentration of glassy IN could be greater than 100 cm^{-3} . Even if half of the accumulation-mode aerosols contain sufficient organics for glass formation, the resulting glassy IN concentration would be 10 cm^{-3} . As shown below, such a large concentration of IN can dominate TTL ice nucleation even if the heterogeneous nucleation supersaturation threshold is close to the homogeneous freezing limit.

As discussed above, the experimental results with mixed ammonium sulfate/organic aerosols indicate that crystalline ammonium sulfate can act as immersion freezing nuclei, with a temperature-dependent nucleation onset ice saturation ratio of about 1.3–1.4 (Schill et al., 2014). The PALMS measurements indicate that the sulfate in most TTL aerosols is neutralized, suggesting the presence of ammonium sulfate in the aerosols. However, the fraction of aerosols with crystalline ammonium sulfate is not known. We assume the range of effective IN concentrations ($10\text{--}200 \text{ L}^{-1}$) used in the simulations below should encompass the potential range of mineral dust or crystalline ammonium sulfate aerosols in the TTL.

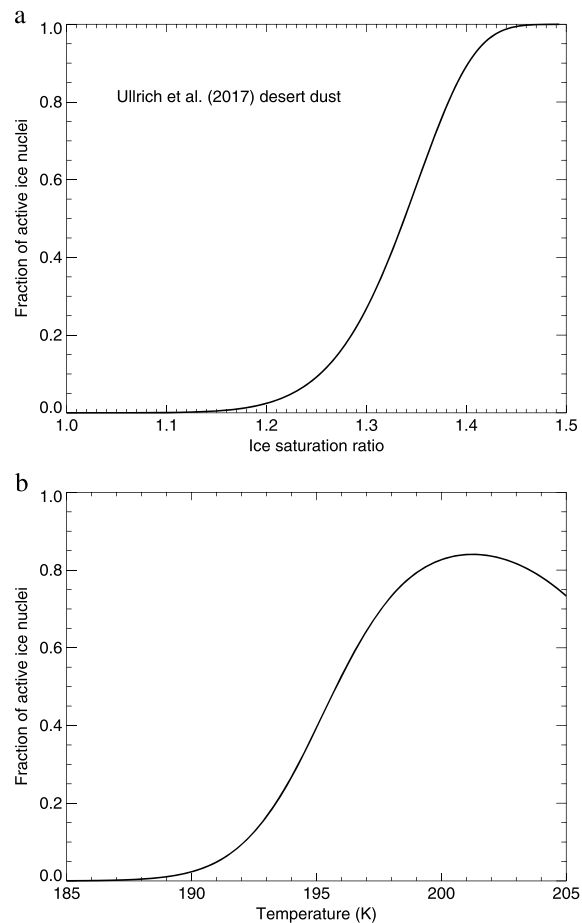


Figure 2. The fraction of dust frozen (a) versus ice saturation ratio at $T = 195$ K and (b) versus temperature at $s_i = 1.3$ based on the expression provided by Ullrich et al. (2017) with a particle radius of $0.3 \mu\text{m}$. Modified coefficients based on low-temperature mineral dust deposition nucleation experiments are used.

5. Simulations of TTL Transport, Ice Nucleation, and Cirrus Evolution

For simulation of the impacts of ice nuclei on TTL cirrus, we use the semi-Lagrangian, one-dimensional cloud model described by Jensen and Pfister (2004) and Ueyama et al. (2014, 2015). Specifically, we run 60-day diabatic back trajectories from 3,780 locations uniformly spaced throughout the tropics. The back trajectories are launched on 1 February 2007 at 372 K potential temperature (about 100 hPa pressure in the tropics during Boreal wintertime). We use ERA-Interim horizontal winds, and vertical motions are diagnosed from diabatic heating rates calculated off-line by Yang et al. (2010) based on climatological TTL temperature, water vapor, and ozone fields as well as cloud properties from satellite measurements. Along each of these trajectories, we extract vertical profiles of temperature from the ERA-Interim fields. The resulting temperature curtains (temperature versus height and time along the trajectories) are used to drive one-dimensional simulations of TTL cirrus formation and water vapor. The model tracks thousands of individual ice crystals to represent the clouds, and physical processes simulated include homogeneous freezing and heterogeneous ice nucleation, sedimentation, deposition growth, and sublimation. Water vapor is calculated on an Eulerian grid with a vertical potential-temperature resolution of 0.4 K.

A number of modeling studies have shown that competition between heterogeneous and homogeneous ice nucleation depends on the cooling rate (e.g., DeMott et al., 1997; Kärcher et al., 2006; Spichtinger et al., 2010). If the cooling driving ice nucleation is relatively slow, then the growth of ice crystals produced by even a small number of IN can quench the rising supersaturation and prevent homogeneous freezing, whereas if the cooling is rapid, then the supersaturation will continue to rise until homogeneous freezing occurs, in which case the numerous ice crystals produced by homogeneous freezing will dominate the cloud. High-frequency waves (periods shorter than about a day) are not resolved in the meteorological analysis fields used to drive

Table 1
List of TTL Cirrus Simulation Sets and Summary of Results

Case	$S_{i,nuc}$	$N_{IN,init}^a$	$N_{IN,30-60d}^b$	$f_{het,cld}^c$	$f_{het,ice}^d$	f_{cld}^e	Median N_{ice}^f	$f_{S_i > 1.4}^g$
Measurements								
ATTREX							59 ⁱ	0.067 ^h
POSIDON							83 ⁱ	0.11 ^h
Model results								
Homfreeze only	1.7	0	0	0	0	0.029	184	0.083
10 cm ⁻³ Glassy sugar/acid IN ^j	1.4	10,000	8,000	0.998	0.999	0.071	109	0.0052
1 cm ⁻³ Glassy sugar/acid IN	1.4	1,000	730	0.98	0.95	0.054	60	0.015
10 cm ⁻³ Glassy SOA IN ^j	1.6	10,000	8,100	0.840	0.700	0.032	125	0.059
1 cm ⁻³ Glassy SOA IN	1.6	1,000	800	0.35	0.080	0.025	117	0.078
10 L ⁻¹ Mineral dust IN ⁱ	1.3	10	4.0	0.18	0.012	0.034	169	0.082
50 L ⁻¹ Mineral dust IN	1.3	50	19	0.60	0.12	0.039	116	0.069
200 L ⁻¹ Mineral dust IN	1.3	200	120	0.86	0.27	0.033	70	0.039

^aInitial ice nuclei concentration. IN and ice crystal concentration units are L⁻¹. ^bIN concentration after 30 days of nucleation scavenging in 60-day simulations. Average over 370–380 K potential temperature, latitude within ±20°. ^cFraction of cloudy grid cells with some fraction of ice produced by heterogeneous nucleation. All simulations results correspond to 30–60 days simulation time, 370–380 K potential temperature. ^dFraction of TTL cirrus ice crystals nucleated heterogeneously. ^eMean TTL cirrus occurrence frequency. ^fMedian ice concentration including $N_{ice} > 15 \text{ L}^{-1}$ corresponding to FCDP measurement threshold. ^gFraction of supersaturated locations with $S_i > 1.4$. ^h $S_i > 1.4$ fraction based on Diode Laser Hygrometer (DLH) water vapor and Meteorological Measurement System (MMS) temperature measurements. ⁱIce concentration from Fast Cloud Droplet Probe (FCDP) measurements. Note that we consider the mineral dust cases also appropriate for ammonium sulfate since the laboratory experiments indicate similar nucleation thresholds. ^j $S_0 = 1.3$, $\alpha = 10$. ^k $S_0 = 1.55$, $\alpha = 30$.

our simulations. We use a wave parameterization to superimpose wave-driven temperature variations on the temperature curtains (Jensen & Pfister, 2004). The parameterization uses 70 distinct frequencies with random phases. As discussed by Ueyama et al. (2015), we also apply the scheme described by Kim and Alexander (2013) to properly interpolate and amplify the waves included in the analysis fields. Recent analyses of super-pressure balloon measurements have constrained the amplitudes of waves in the tropical tropopause region to about 0.7 K (Podglajen et al., 2016; Schoeberl et al., 2017), and we have increased the wave amplitudes in our parameterization accordingly. As shown by Jensen et al. (2010) and Spichtinger and Krämer (2013), waves with very short periods can terminate homogeneous freezing events and result in relatively low ice concentrations. This effect is included in the simulations presented here; however, as shown by Jensen et al. (2016), this high-frequency wave-quenching effect has negligible impact on cirrus ice concentrations when realistic wave spectra are used.

As described by Ueyama et al. (2014, 2015), the influence of deep convection on the vertical profile of humidity in the model is treated by tracing the trajectories through geostationary-satellite infrared fields of convective cloud top height. Whenever the trajectories pass through convective clouds with heights extending into the TTL, we set the humidity profile up to the cloud top to the ice saturation mixing ratio. The infrared cloud top heights are adjusted to correct for the known 1- to 2-km low bias (Sherwood et al., 2004). We also detrain ice crystals at the convective influence locations. Assuming that deep convection is the primary source of ice nuclei to the TTL, we also include replenishment of IN at the convective influence locations in the simulations presented here. Specifically, we restore the IN concentration and size distribution to the assumed initial conditions up to the convective cloud top heights. This approach would be reasonable if the background aerosol properties result from a combination of convective sources and nucleation scavenging by in situ cirrus.

The water vapor profiles in these simulations are initialized with Microwave Limb Sounder observations; however, sensitivity experiments indicate that changing the initial humidity profiles has no significant impact on the model results after the first few weeks of the 60-day simulations. The simulated TTL cloud frequencies and water vapor concentrations agree well with satellite measurements (Ueyama et al., 2015).

6. Results

We have run sets of simulations with a number of assumptions about TTL IN abundance and efficacy (see Table 1). As an extreme case with abundant glassy IN, we assume 50% of the 20-cm⁻³ TTL accumulation-mode aerosols are glassy, resulting in a glassy aerosol concentration of 10 cm⁻³. We have used parameters in the

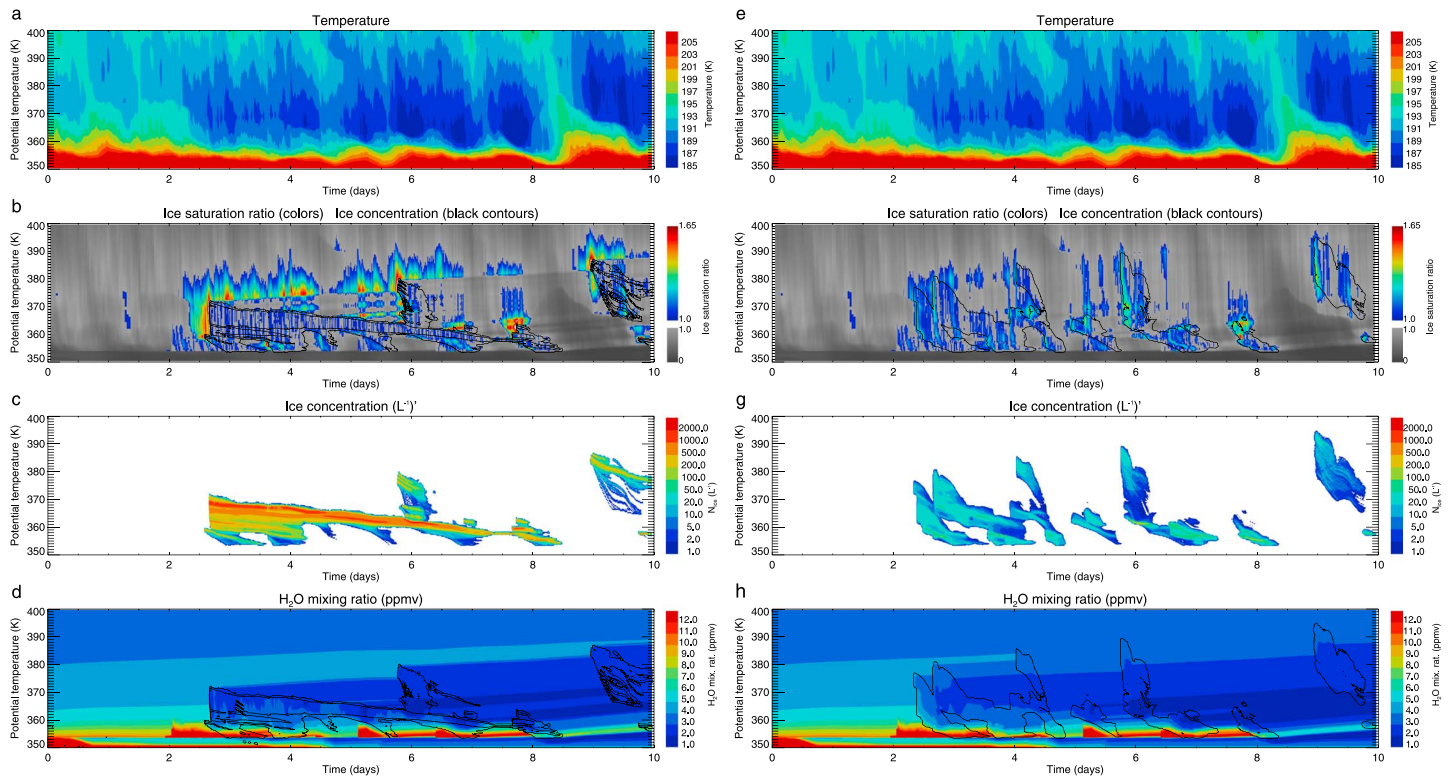


Figure 3. Examples of cloud formation by homogeneous nucleation (left column) and heterogeneous nucleation ($N_{IN} = 65 \text{ L}^{-1}$, right column) in the first 10 days of a particular curtain simulation. Fields shown versus time and height are temperature (a and e), ice saturation ratio (b and f), ice concentration (c and g), and water vapor mixing ratio (d and h). Ice concentrations are also shown with black contours on panels b, d, f, and h for reference.

nucleation model corresponding to relatively effective glassy IN based on the laboratory experiments with simple sugars as well as parameters for IN activation just before homogeneous freezing threshold based on the laboratory experiments with SOA-like aerosols. Note that only a small fraction of the glassy IN will actually nucleate ice crystals (see Figure 1). We use log-normal size distribution parameters for the glassy IN appropriate for the accumulation mode ($r_0 = 0.2 \mu\text{m}$, $\sigma = 1.6$). We have also run sets of simulations assuming that only 5% of the accumulation-mode aerosols (1 cm^{-3}) are glassy and available for heterogeneous nucleation. It is also possible that the ultrafine aerosols contain organics and are glassy, which would provide an extremely abundant source of IN. However, as shown below, even 1- to 10-cm^{-3} glassy organic-containing IN can dominate the cirrus properties. The IN and aqueous aerosol concentrations are assumed to be initially uniformly distributed in height.

As discussed above the TTL mineral dust concentration is poorly constrained because of the sparse measurements. We have run simulations with initial TTL dust concentrations of 10, 50, and 200 L^{-1} . The latter values are likely higher than typical TTL dust concentrations, but the assumed range is useful for demonstrating the potential impacts of relatively abundant effective IN (such as ammonium sulfate) on TTL cirrus. Note that, as shown below, nucleation scavenging reduces dust IN concentrations by about a factor of 2 after a few weeks of simulation time. The depleted dust IN concentrations are more appropriate for comparison with PALMS TTL dust concentrations (about $5\text{--}10 \text{ L}^{-1}$). The cases with initial dust concentrations of 50 and 200 L^{-1} (25 and 100 L^{-1} after scavenging) are still excessive compared to the PALMS measurements. As discussed above, the concentration of crystalline ammonium sulfate particles (which have a similar supersaturation threshold for ice nucleation as dust particles) in the TTL is unknown. However, since the PALMS measurements indicate that most of the aerosols are at least partially neutralized, ammonium sulfate IN could be quite abundant.

Figure 3 shows the contrast between simulated clouds formed by homogeneous and heterogeneous freezing (with 65 L^{-1} effective mineral dust IN) during the first 10 days of a particular temperature curtain. In this example, homogeneous freezing produces a layer of ice concentrations approaching $1,000 \text{ L}^{-1}$, resulting in relatively small ice crystals that sediment slowly (Figure 3c), whereas in the heterogeneous nucleation case,

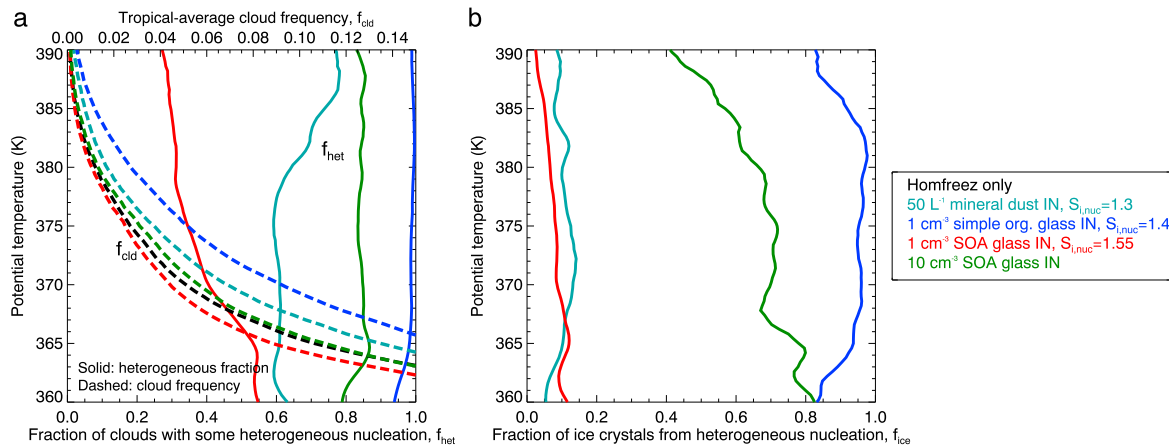


Figure 4. Tropical mean statistics of cloud properties based on 3,780 curtain simulations. Panels show (a) mean fraction of clouds including ice generated by heterogeneous nucleation during the last 30 days of the 60-day simulations (solid curves), and (b) mean fraction of TTL cirrus ice crystals from heterogeneous nucleation. The dotted curves in panel (a) show the tropical mean cloud fraction. Black curves: baseline set of simulations with only homogeneous freezing; cyan curves: initial mineral dust IN concentration of 50 L⁻¹; blue curves: initial effective glassy IN concentration of 1 cm⁻³ with nucleation thresholds corresponding to laboratory experiments with simple sugars/acids; red curves = 1 cm⁻³ ineffective glassy IN with nucleation thresholds corresponding to laboratory experiments with SOA-like aerosols; green curves = 10 cm⁻³ ineffective glassy IN. See Table 1 for summary of results. TTL = Tropical Tropopause Layer; SOA = secondary organic aerosols; IN = ice nuclei.

ice concentrations are limited by the IN abundance, the ice crystals grow larger, and the cloud element lifetimes are more often limited by sedimentation (Figure 3g). As expected, higher supersaturations are reached before homogeneous freezing ice nucleation occurs (Figure 3b) than in the case with IN available (Figure 3f). In both cases, the clouds formed effectively dehydrate the TTL, and the differences in the water vapor concentrations after 10 days between the homogeneous and heterogeneous nucleation simulations are subtle (Figures 3d and 3h). This is consistent with the results of Ueyama et al. (2015), who showed that the impact of including heterogeneous ice nuclei on 100 hPa water vapor is small.

Inclusion of ice nuclei can either increase or decrease cloud occurrence frequencies. The lower supersaturation threshold for activation of IN implies that IN can allow clouds to form in locations where the supersaturation threshold for homogeneous freezing might never be reached. On the other hand, cirrus produced by heterogeneous freezing tend to have lower concentrations of larger ice crystals, resulting in more rapid sedimentation removal of the crystals. As shown below, the overall impact of assumed ice nuclei properties on tropical mean TTL cirrus occurrence frequencies can be significant but complicated, with dependencies on the assumed IN efficiency and abundance.

Figure 4 shows the relative importance of heterogeneous and homogeneous ice nucleation on a statistical mean basis in sets of simulations with different assumptions about glassy particles or mineral dust acting as ice nuclei. Both the fraction of clouds with some contribution from heterogeneous freezing (f_{het} , Figure 4a) and the fraction of ice crystals produced by heterogeneous freezing (f_{ice} , Figure 4b) are shown. Median bulk cloud properties from the different sets of simulations are provided in Table 1. The sensitivities of median TTL ice concentration and mean TTL cloud fraction to IN concentration are summarized in Figure 5. Using glassy organic IN with a low supersaturation threshold ($S_{i,nuc} \approx 1.4$ corresponding to simple sugar/acid laboratory results, blue curves) with concentrations ≥ 1 cm⁻³ results in overwhelming dominance of heterogeneous nucleation over homogeneous freezing. With the higher glassy IN supersaturation threshold ($S_{i,nuc} \approx 1.6$, corresponding to SOA-like aerosol laboratory results), heterogeneous nucleation is still dominant with 10 cm⁻³ glassy aerosols (green curves), but with only 1 cm⁻³ glassy aerosols (red curves), both heterogeneous nucleation and homogeneous freezing both contribute significantly to TTL ice production. Note again that in the simulations with abundant glassy IN, nucleation usually only occurs on a small fraction of the available IN. As a result, the ice nuclei population is not significantly depleted by nucleation scavenging.

The simulated TTL-mean cirrus occurrence frequency (f_{cld} , dashed curves in Figure 4a) varies by nearly a factor of three (0.025–0.0071) with different assumptions about ice nuclei (see Table 1 and Figure 5), and the dependence on assumed IN properties is complicated. For different assumed IN supersaturation thresholds and different IN concentrations, the inclusion of IN can either increase or decrease cloud frequency. Inclusion

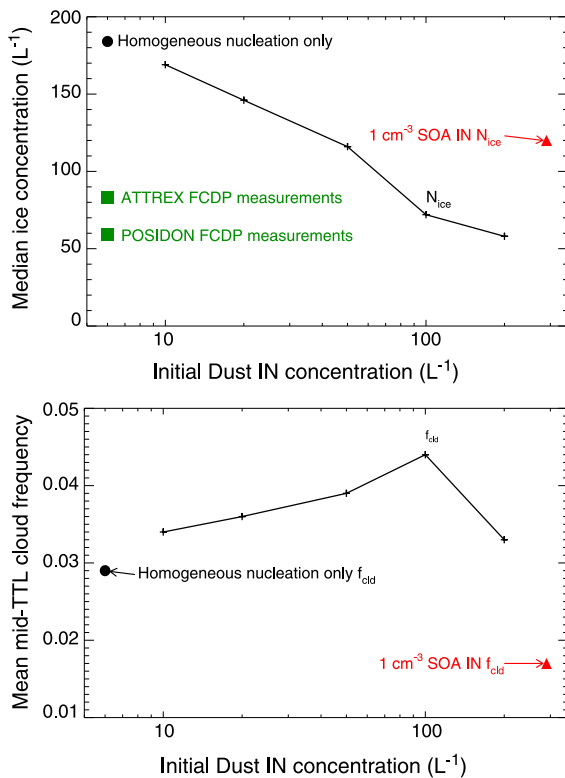


Figure 5. Median upper TTL (370–380 K potential temperature) ice concentration (top panel) and mean TTL cloud frequency (bottom panel) are plotted versus mineral dust IN concentration (black curves). The ice concentration and cloud fraction from simulations with only homogeneous freezing are shown by black circles. The ice concentration and cloud fraction from simulations with 1 cm⁻³ glassy SOA particles are indicated by red triangles. Also shown are the median TTL ice concentrations measured by the FCDP probe during ATTREX and POSIDON (green squares). TTL = Tropical Tropopause Layer; SOA = secondary organic aerosols; FCDP = Fast Cloud Droplet Probe; ATTREX = Airborne Tropical Tropopause Experiment; POSIDON = Pacific Oxidants, Sulfur, Ice, Dehydration, and cONvection experiment.

distributions of ice concentration (and supersaturation, discussed below) differ significantly between the two campaigns. The higher ice concentrations observed during POSIDON could be related to stronger wave activity associated with stronger convection than during ATTREX. On the other hand, the aircraft sampling is necessarily limited, and these differences could just be associated with sampling bias; that is, the POSIDON flights may have just spent more time in regions with high ice concentrations and supersaturations. The median concentrations larger than the FCDP threshold of 15 L⁻¹ are provided in Table 1. Note that the median concentrations including values lower than 15 L⁻¹ (which occur frequently) are considerably lower.

As discussed by Jensen et al. (2016), simulations with only homogeneous freezing ice nucleation and realistic representations of high-frequency waves (black curve in Figure 6a) tend to produce higher ice concentrations than indicated by the measurements. With the comparison limited to ice concentrations greater than 15 L⁻¹, the discrepancy is a factor of 2–3 in terms of median ice concentration (Table 1). With 5% of the accumulation-mode aerosols (1 cm⁻³, blue curve) effective glassy IN, the median ice concentration is reduced by a factor of 2, and ice concentrations exceeding a few thousands per liter are absent (in contrast to the observations). Abundant glassy SOA-like particles (concentration of 10 cm⁻³, green curve) improve agreement with the measured ice concentration frequency distribution. Recall that the nucleation-model parameters used for glassy organic particles (based on laboratory experiments, see section 5) result in small fractions of available glassy particles active as IN. With 1 cm⁻³ glassy SOA particles (red curve), homogeneous freezing still occurs much of the time, but the occurrence of very high ice concentrations is reduced significantly.

of IN tends to increase TTL cirrus frequencies compared to the homogeneous freezing only case (black curve in Figure 4; see also Figure 5), particularly if the IN have a low supersaturation threshold for ice nucleation. The set of simulations with 1 cm⁻³ glassy IN having a supersaturation threshold just below the homogeneous nucleation threshold has the lowest occurrence frequency because the supersaturation required for ice nucleation is not low enough to enhance cloud frequency, but the ice concentrations are reduced by heterogeneous nucleation (resulting in larger ice crystals that sediment out of the clouds faster).

Initializing the simulations with 10 L⁻¹ dust IN has little impact on the simulated cloud properties (compared to the homogeneous freezing only case) (Table 1) because in general too few ice crystals are nucleated heterogeneously to quench the rising supersaturation and homogeneous freezing dominates TTL ice production. The influence of dust particles is further reduced by the fact that the IN are depleted by nucleation scavenging. After 30 days, the TTL-mean dust IN concentration is reduced by about 50%. With 50 L⁻¹ dust IN at the start of the simulations, heterogeneous nucleation contributes to most TTL cirrus clouds, but more than 90% of the ice crystals still come from homogeneous freezing (cyan curves in Figure 4). TTL cirrus occurrence frequencies are relatively high in this case (see Figure 5) because the dust IN allow cloud formation at low supersaturation, but homogeneous freezing still dominates the mean ice concentration, resulting in numerous small crystals and relatively long-lived clouds. With an initial effective IN concentration of 200 L⁻¹, heterogeneous nucleation contributes to most cloud events and about a quarter of all TTL ice crystals are generated heterogeneously ($f_{\text{het}} = 0.27$ in Table 1). Increasing the IN concentration from 50 to 200 L⁻¹ reduces cloud frequency (Figure 5), because the more abundant IN reduce ice concentrations and increase ice crystal sizes, resulting in more rapid sedimentation loss.

The impact of different assumptions about heterogeneous IN on frequency distributions of TTL ice concentrations is shown in Figure 6a (see also Figure 5). For comparison, the frequency distributions of ice concentrations measured with the FCDP probe during ATTREX and POSIDON are also shown (thick black curves with symbols; see Woods et al., 2018 for description of ATTREX TTL cirrus measurements). The frequency distributions of ice concentration (and supersaturation, discussed below) differ significantly between the two campaigns.

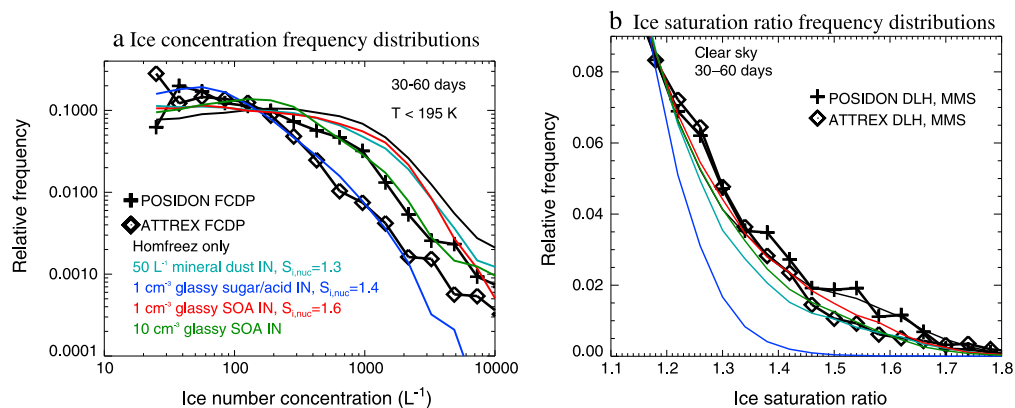


Figure 6. Frequency distributions of (a) TTL cirrus ice concentrations and (b) clear-sky ice supersaturation are shown. The values on the ordinate in panel (b) indicate the fraction of time with a given ice saturation ratio divided by the total time with saturation ratio greater than 1. The thick black curve with + symbols is based on the extensive data set of FCDP measurements in TTL cirrus ice concentration (a), and DLH and MMS measurements of ice saturation ratio (b) from the ATTREX and POSIDON campaigns. Colors are the same as in Figure 4. The median TTL ice concentrations and fractions of time with supersaturation greater than 1.4 are provided in Table 1. TTL = Tropical Tropopause Layer; FCDP = Fast Cloud Droplet Probe; DLH = Diode Laser Hygrometer; MMS = Meteorological Measurement System; ATTREX = Airborne Tropical Tropopause Experiment; POSIDON = Pacific Oxidants, Sulfur, Ice, Dehydration, and cONvection experiment.

In simulations with mineral dust IN included, the median TTL ice concentration is lower than in the homogeneous freezing-only case, and the ice concentration steadily decreases with increasing initial dust IN concentration up to 200 L^{-1} (Figure 5). An abundance of about $50\text{--}100 \text{ L}^{-1}$ of effective IN (such as mineral dust or ammonium sulfate) can greatly improve agreement between measured and simulated ice concentrations.

In principle, the presence of IN that nucleate ice at lower supersaturations than that required for homogeneous freezing will affect the occurrence frequency of clear-sky supersaturation, and comparison with observations might be used to determine which nucleation mechanism dominates ice production (Cziczo et al., 2013). Figure 6b shows the frequency distributions of clear-sky supersaturation in the simulations with different ice nuclei specifications. Also shown are the distributions of clear-sky supersaturation based on the ATTREX and POSIDON DLH H_2O measurements and the MMS pressure and temperature measurements. The fractions of time that the ice saturation ratio exceeds 1.4 divided by the fraction of time with supersaturation for the observations and simulations are provided in Table 1. The agreement between observed and simulated supersaturation statistics is quite good even with only homogeneous freezing included. It is worth noting that even in the homogeneous freezing-only case, supersaturations approaching the threshold for homogeneous freezing occur rarely (less than a few percent of the time). The buildup of supersaturation caused by wave-driven cooling tends to be rapid, and the ice supersaturation decreases rapidly once ice nucleation occurs since homogeneous freezing often produces large concentrations of ice crystals.

Inclusion of relatively ineffective, SOA-like glassy IN has only modest impact on the supersaturation statistics, which makes sense since the assumed threshold for IN activation is close to the threshold for homogeneous freezing. Inclusion of effective glassy IN substantially reduces the occurrence frequency of large supersaturations, resulting in clear disagreement with the measured supersaturation frequency distributions. As discussed above, the uncertainties in water vapor and temperature measurements broaden the observed ice saturation ratio frequency distributions slightly, but the discrepancy with the simulations using simple sugar/acid organic nucleation parameters still stands out distinctly.

As discussed above, initializing the model with $10\text{--}50 \text{ L}^{-1}$ mineral dust IN has little impact on mean TTL ice concentrations (Table 1) during the final 30 days of the 60-day simulations. The limited impact is partly a result of the fact that nucleation scavenging reduces the dust IN concentration by a factor of 2. Including $10\text{--}50 \text{ L}^{-1}$ dust IN has negligible impact on supersaturation statistics. Increasing the dust IN concentration to 200 L^{-1} decreases the mean ice concentration by a factor of 2 and reduces the occurrence frequency of large supersaturation well below the range indicated by the observations (Table 1).

6.1. Discussion of Uncertainties

As discussed by Ueyama et al. (2015), the simulations of TTL transport, water vapor, and cirrus used here are subject to a number of uncertainties, which raises the question of robustness of the results presented. Since our focus is on cloud processes, with an emphasis on the competition between homogeneous and heterogeneous ice nucleation, the most important issue is the distribution of cooling rates driving nucleation. Faster cooling rates will tend to produce higher supersaturations, driving more frequent homogeneous freezing and higher ice crystal concentrations. In the upper troposphere, cooling rates are dominated by waves spanning a wide range of spatial and temporal scales. The approach used here involves superposition of a spectrum of high-frequency waves not resolved in the meteorological analysis. The wave properties are constrained by superpressure balloon measurements (Podglajen et al., 2016; Schoeberl et al., 2017), but limited information is available about the height dependence and regional variability of wave amplitudes. As expected, decreasing the wave amplitudes results in somewhat greater dominance of heterogeneous freezing. In a set of simulations with 1 cm^{-3} SOA-like glassy IN using wave amplitudes reduced by a factor of 2, the fraction of TTL ice crystals produced by heterogeneous nucleation increases about 5%, and the median ice concentration decreases about 5% compared to the set of simulations with the baseline wave amplitudes. Increasing the high-frequency wave amplitudes by a factor of 2 decreases the fractions of TTL ice concentrations from heterogeneous nucleation by about 15%, and increases the median ice concentrations about 5%. We conclude that the competition between heterogeneous and homogeneous nucleation is not strongly sensitive to the specified high-frequency wave amplitudes. Note that completely omitting high-frequency wave temperature perturbations would dramatically change the simulated ice concentrations and result in much greater dominance of heterogeneous nucleation.

As noted by Lin et al. (2005) and Murphy (2014), high vertical resolution is required to properly simulate homogeneous nucleation in one-dimensional models. In the simulations described above, we used a potential temperature grid with a vertical grid spacing of 0.4 K in the Eulerian representation of water vapor. Ice crystals are treated with a purely Lagrangian approach. To evaluate the vertical-resolution dependence of our results, we have doubled the number of vertical grid levels and repeated the set of simulations with 1 cm^{-3} SOA-like glassy IN. The increased vertical resolution changes the cloud frequencies, median ice concentrations, and relative contributions of homogeneous and heterogeneous nucleation by no more than about 10%. This test suggests that 0.4 K potential-temperature resolution is sufficient for the purposes of this study.

A number of issues that can affect the competition between homogeneous and heterogeneous nucleation, such as preactivation and the coexistence of a variety of types of IN, have not been addressed here. The purpose of this study was to explore sensitivities with a range of possible IN types and concentrations based on our current knowledge of heterogeneous nucleation at cold temperatures and limited information about aerosol composition in the TTL. Another issue not addressed here in detail is the sensitivity to the source of IN from deep convection. Very little is currently known about what types of aerosols survive transport through deep convection and get detrained in the TTL.

7. Summary and Discussion

In this study, we developed a simple framework for representing the supersaturation and temperature dependence of heterogeneous nuclei at low temperatures. Parameter values appropriate for the efficiency of glassy organic-containing aerosols and mineral dust aerosols were specified based on recent laboratory experiments. We note also that laboratory experiments indicate that crystalline ammonium sulfate can also be an effective ice nucleus with activation at supersaturations similar to mineral dust particles. The heterogeneous nucleation parameterization was applied in a detailed model of TTL transport and cirrus formation. Ice nucleation, deposition growth, and sedimentation were treated explicitly, and high-frequency wave temperature perturbations were included with wave amplitudes constrained by recent superpressure balloon measurements. The impacts of different assumptions about glassy aerosol and dust particle ice nuclei abundance and efficiency on the competition between heterogeneous and homogeneous ice nucleation in TTL cirrus were evaluated. In addition, the simulated impacts of IN on TTL cirrus occurrence frequency, and the statistics of ice concentration, extinction, and supersaturation were quantified. The simulation results were compared with recent high-altitude aircraft measurements of TTL cirrus microphysical properties and supersaturation with respect to ice. The key findings are summarized as follows:

1. Given the laboratory experiments indicating that organic-containing aerosols transition to a glassy state at TTL temperatures along with the field measurements indicating that most TTL accumulation-mode

aerosols contain substantial mass fractions of organics, it seems plausible that a large fraction of the TTL accumulation-mode aerosols could be glassy. The simulations presented here indicate that if even 1% of the glassy aerosols serve as effective IN (corresponding to laboratory results with simple sugars/acids), then large ice concentrations and high supersaturations would occur much less frequently than indicated by the observations. The conflict between simulated absence of large supersaturations in the sugar/acid organic case and the occasional occurrence of large supersaturations in the observations is pronounced and would seem to rule out this scenario. The model/observations discrepancy would be even worse if TTL glassy organic aerosols were preactivated by previous cloud cycling such that they were active as IN at very low supersaturations. The comparison between observed and simulated ice concentration and supersaturation statistics is much better if we use ice nuclei specifications (high supersaturation thresholds) corresponding to the laboratory experiments with SOA-like aerosols, which should be better proxies for organic aerosols in the TTL.

2. Inclusion of plausible ice nuclei properties and abundances (based on laboratory ice nucleation experiments and field measurements of aerosol composition) can have substantial impacts on TTL cirrus occurrence frequency, but the cloud frequency can increase or decrease depending on the specified threshold supersaturation for activation of IN and the abundance of IN. The range of TTL cirrus frequencies from sets of simulations with different IN specifications can be as much as a factor of 2–3. The occurrence frequency is highest when the ice nuclei promote nucleation at relatively low supersaturation but are not so abundant as to substantially reduce ice concentrations. The cloud frequencies are lowest when the IN supersaturation threshold is similar to the homogeneous freezing threshold and the IN are abundant enough to reduce ice concentrations and thereby reduce cloud lifetimes.
3. The laboratory experiments also indicate that mineral dust or crystalline ammonium sulfate are viable TTL ice nuclei. However, the limited available field measurements suggest TTL mineral dust particle concentrations are very low (on the order of 10 L^{-1} or less). The simulations using dust particle nucleation parameters indicate that such low IN concentrations would have negligible impact on TTL cirrus microphysical properties or supersaturation statistics. With 50 L^{-1} dust IN, the TTL cirrus occurrence frequency is increased, but homogeneous freezing still dominates the ice concentration statistics. Increasing the concentration of effective IN to 200 L^{-1} substantially reduces ice concentrations and thereby reduces cloud frequencies. However, in this case the frequency of large supersaturation occurrence is reduced well below the observed values. The latter result suggests that an abundant population ($> 200 \text{ L}^{-1}$) of effective TTL IN from crystalline ammonium sulfate is unlikely.
4. The simulations with limited concentrations of IN specified in the initial conditions indicate that nucleation scavenging is an important process in the stable, slowly ascending TTL. With initial mineral dust concentrations of $10\text{--}200 \text{ L}^{-1}$, nucleation scavenging reduces the IN concentration by about a factor of 2 after a few weeks of simulation time. This result suggests that if effective IN are injected into the lower-middle TTL by deep convection, the IN concentration may be substantially reduced over time as air parcels slowly ascend toward the cold-point tropopause where final dehydration of air entering the stratosphere occurs. The nucleation-scavenging process is important to include in global-model simulations of mineral dust and other particle types that are effective IN.

The extensive laboratory research summarized in section 2 has advanced our understanding of aerosol physical state and ice nucleation efficiency at low temperatures, and the simulations presented here suggest significant potential impacts on TTL cirrus occurrence and microphysical properties. However, we emphasize that large uncertainties remain in the abundance and effectiveness of TTL ice nuclei, and none of the relatively simple ice nuclei scenarios presented here produces simulated ice concentrations *and* supersaturation frequencies in complete agreement with the observations (Table 1). Even if the balance between heterogeneous and homogeneous nucleation were constrained in the current atmosphere, the response of TTL cirrus occurrence frequency and cloud microphysical properties to changing IN would have complicated dependencies on the altered IN abundance and efficacy. Important phenomena and processes such as small-scale wave-driven temperature perturbations and ice nucleation necessarily need to be parameterized in global models, and some of the important effects are currently not included. Given the assortment of uncertainties, meaningful estimates of TTL aerosol-cirrus indirect effects on radiative forcing (let alone radiative forcing estimates for geoengineering scenarios with modified IN) are likely not possible at this time.

The remaining uncertainties in our understanding of TTL ice nucleation stem primarily from the dearth of direct field measurements of TTL aerosol composition and physical state. As discussed in section 3, the only

measurements of TTL aerosol composition were made with the PALMS instrument on high-altitude aircraft flights from Costa Rica during Boreal wintertime. It is unknown how representative these measurements are of the global TTL aerosol properties. Future measurements of TTL aerosol composition and physical state would help constrain the role of heterogeneous nucleation in the current atmosphere as well as the potential for TTL cirrus modification resulting from changes in ice nuclei abundance.

Acknowledgments

This work was supported by NASA's Airborne Tropical Tropopause Experiment project. We thank Ben Murray, Ottmar Möhler, Corinna Hoose, and Margaret Tolbert for helpful discussions. Data used in this study can be accessed at the NASA Earth Sciences Project Office archive (espoarchive.nasa.gov).

References

- Abbatt, J. P. D., Benz, S., Cziczo, D. J., Kanji, Z., Lohmann, U., & Möhler, O. (2006). Solid ammonium sulfate aerosols as ice nuclei: A pathway for cirrus formation. *Science*, *313*, 1770–1773.
- Baker, B., Mo, Q., Lawson, R. P., Korolev, A., & O'Connor, D. (2009). Drop size distributions and the lack of small drops in RICO rain shafts. *Journal of the Atmospheric Sciences*, *48*, 616–623.
- Barahona, D., & Nenes, A. (2011). Dynamical states of low temperature cirrus. *Atmospheric Chemistry and Physics*, *11*, 3757–3771.
- Baustian, K. J., Wise, M. E., Jensen, E. J., Schill, G. P., Freedman, M. A., & Tolbert, M. A. (2013). State transformations and ice nucleation in amorphous (semi-)solid organic aerosol. *Atmospheric Chemistry and Physics*, *13*, 5615–5628.
- Baustian, K. J., Wise, M. E., & Tolbert, M. A. (2009). Depositional ice nucleation on solid ammonium sulfate and glutaric acid particles. *Atmospheric Chemistry and Physics*, *9*, 20,929–20,977.
- Berkemeier, T., Shiraiwa, M., Pöschl, U., & Koop, T. (2014). Competition between water uptake and ice nucleation by glassy organic aerosol particles. *Atmospheric Chemistry and Physics*, *14*, 12,513–12,531.
- Bodsworth, A., Zobrist, B., & Bertram, A. K. (2010). Inhibition of efflorescence in mixed organic-inorganic particles at temperatures less than 250 K. *Physical Chemistry Chemical Physics*, *12*, 12,259–12,266.
- Brock, C. A., Hamill, P., Wilson, J. C., Jonsson, H. H., & Chan, K. R. (1995). Particle formation in the upper tropical troposphere: A source of nuclei for the stratospheric aerosol. *Science*, *270*(L05803), 1650–1653.
- Chen, Y., Kreidenweis, S. M., McInnes, L. M., Rogers, D. C., & DeMott, P. J. (1998). Single particle analyses of ice nucleating aerosols in the upper troposphere and lower stratosphere. *Geophysical Research Letters*, *25*, 1391–1394.
- Cziczo, D. J., & Froyd, K. D. (2014). Sampling the composition of cirrus ice residuals. *Atmospheric Research*, *142*, 15–31.
- Cziczo, D. J., Froyd, K. D., Hoose, C., Jensen, E. J., Diao, M., Zondlo, M. A., et al. (2013). Clarifying the dominant sources and mechanisms of cirrus cloud formation. *Science*, *340*, 1320–1324.
- Cziczo, D. J., Stetzer, O., Worringer, A., Ebert, M., Weinbruch, S., Kamphus, M., et al. (2009). Inadvertent climate modification due to anthropogenic lead. *Nature Geoscience*, *2*, 333–336.
- DeMott, P. J. (1995). Quantitative descriptions of ice formation mechanisms of silver iodide-type aerosols. *Atmospheric Research*, *38*, 63–99.
- DeMott, P. J., Prenni, A. J., Liu, X., Kreidenweis, S. M., Petters, M. D., Twohy, C. H., et al. (2010). Predicting global atmospheric ice nuclei distributions and their impacts on climate. *Proceedings of the National Academy of Sciences of the United States of America*, *107*, 11,217–11,222.
- DeMott, P. J., Rogers, D. C., & Kreidenweis, S. M. (1997). The susceptibility of ice formation in upper tropospheric clouds to insoluble aerosol components. *Journal of Geophysical Research*, *102*, 19,575–19,584.
- Field, P. R., Heymsfield, A. J., & Bansemmer, A. (2006). Shattering and particle interarrival times measured by optical array probes in ice clouds. *Journal of Atmospheric and Oceanic Technology*, *23*, 1357–1371.
- Forster, P. M. F., & Shine, K. P. (2002). Assessing the climate impact of trends in stratospheric water vapor. *Geophysical Research Letters*, *29*(6), 11086. <https://doi.org/10.1029/2001GL013909>
- Froyd, K. D., Murphy, D. M., Lawson, P., Baumgardner, D., & Herman, R. L. (2010). Aerosols that form subvisible cirrus at the tropical tropopause. *Atmospheric Chemistry and Physics*, *10*, 209–218.
- Froyd, K. D., Murphy, D. M., Sanford, T. J., Thomson, D. S., Wilson, J. C., Pfister, L., & Lait, L. (2009). Aerosol composition of the tropical upper troposphere. *Atmospheric Chemistry and Physics*, *9*, 4363–4385.
- Gasparini, B., & Lohmann, U. (2016). Why cirrus cloud seeding cannot substantially cool the planet. *Journal of Geophysical Research: Atmospheres*, *121*, 4877–4893. <https://doi.org/10.1002/2015JD024666>
- Gettelman, A., Morrison, H., Santos, S., Bogenschutz, P., & Caldwell, P. M. (2015). Advanced two-moment bulk microphysics for global models. Part II: Global model solutions and aerosol-cloud interactions. *Journal of Climate*, *28*, 1288–1307.
- Herbert, R. J., Murray, B. J., Whale, T. F., Dobbie, S. J., & Atkinson, J. D. (2014). Representing time-dependent freezing behaviour in immersion mode ice nucleation. *Atmospheric Chemistry and Physics*, *14*, 8501–8520.
- Hoose, C., & Möhler, O. (2012). Heterogeneous ice nucleation on atmospheric aerosols: A review of results from laboratory experiments. *Atmospheric Chemistry and Physics*, *12*, 9817–9854.
- Ignatius, K., Thomas, B. K., Emma, J., Leonid, N., Claudia, F., Hamish, G., et al. (2016). Heterogeneous ice nucleation of viscous secondary organic aerosol produced from ozonolysis of alpha-pinene. *Atmospheric Chemistry and Physics*, *16*, 6495–6509.
- Jensen, E. J., Diskin, G., Lawson, R. P., Lance, S., Bui, T. P., Hlavka, D., et al. (2013). Ice nucleation and dehydration in the tropical tropopause layer. *Proceedings of the National Academy of Sciences of the United States of America*, *110*(6), 2041–2046. <https://doi.org/10.1073/pnas.1217104110>
- Jensen, E. J., Lawson, P., Baker, B., Pilon, B., Mo, Q., Heymsfield, A., et al. (2009). On the importance of small ice crystals in tropical anvil cirrus. *Atmospheric Chemistry and Physics*, *9*, 5519–5537.
- Jensen, E. J., & Pfister, L. (2004). Transport and freeze-drying in the tropical tropopause layer. *Journal of Geophysical Research*, *109*, D02207. <https://doi.org/10.1029/2003JD004022>
- Jensen, E. J., Pfister, L., Bui, T.-P., Lawson, P., & Baumgardner, D. (2010). Ice nucleation and cloud microphysical properties in tropical tropopause cirrus. *Atmospheric Chemistry and Physics*, *10*, 1369–1384.
- Jensen, E. J., Pfister, L., Jordan, D., Bui, T. P., Ueyama, R., Singh, H., et al. (2017). The NASA airborne tropical tropopause experiment (ATTREX): High-altitude aircraft measurements in the tropical Western Pacific. *Bulletin of the American Meteorological Society*, *1*, 129–143. <https://doi.org/10.1175/BAMS-D-14-00263.1>
- Jensen, E. J., Toon, O. B., Tabazadeh, A., Sachse, G. W., Anderson, B. E., Chan, K. R., et al. (1998). Ice nucleation processes in upper tropospheric wave-clouds observed during success. *Geophysical Research Letters*, *25*, 1363–1366.
- Jensen, E. J., Ueyama, R., Pfister, L., Bui, T. V., Lawson, R. P., Woods, S., et al. (2016). On the susceptibility of cold tropical cirrus to ice nuclei abundance. *Journal of the Atmospheric Sciences*, *73*, 2445–2464. <https://doi.org/10.1175/JAS-D-15-0274.1>
- Kärcher, B. (2004). Cirrus clouds in the tropical tropopause layer: Role of heterogeneous ice nuclei. *Geophysical Research Letters*, *31*, L12101. <https://doi.org/10.1029/2004GL019774>

- Kärcher, B. (2017). Cirrus clouds and their response to anthropogenic activities. *Current Climate Change Reports*, 3, 45–57. <https://doi.org/10.1007/s40641-017-0060-3>
- Kärcher, B., Hendricks, J., & Lohmann, U. (2006). Physically based parameterization of cirrus cloud formation for use in global atmospheric models. *Journal of Geophysical Research*, 111, D01205. <https://doi.org/10.1029/2005JD006219>
- Kärcher, B., & Lohmann, U. (2003). A parameterization of cirrus cloud formation: Heterogeneous freezing. *Journal of Geophysical Research*, 108(D14), 4402. <https://doi.org/10.1029/2002JD003220>
- Kim, J.-E., & Alexander, M. J. (2013). A new wave scheme for trajectory simulations of stratospheric water vapor. *Geophysical Research Letters*, 13, 5286–5290. <https://doi.org/10.1002/grl.50963>
- Knopf, D. A., & Alpert, P. A. (2013). A water activity based model of heterogeneous ice nucleation kinetics for freezing of water and aqueous solution droplets. *Faraday Discussions*, 165, 513–534.
- Koop, T., Bookhold, J., Manabu, S., & Pöschl, U. (2011). Glass transition and phase state of organic compounds: Dependency on molecular properties and implications for secondary organic aerosols in the atmosphere. *Physical Chemistry Chemical Physics*, 13, 19,238–19,255.
- Koop, T., Luo, B., Tsias, A., & Peter, T. (2000). Water activity as the determinant for homogeneous ice nucleation in aqueous solutions. *Nature*, 406, 611–614.
- Ladino, L. A., Zhou, S., Yakobi-Hancock, J. D., Aljawhary, D., & Abbatt, J. P. D. (2014). Factors controlling the ice nucleating abilities of aliphatic SOA particles. *Journal of Geophysical Research: Atmospheres*, 119, 9041–9051. <https://doi.org/10.1002/2014JD021578>
- Lawson, R. P. (2011). Effects of ice particles shattering on the 2D-S probe. *Atmospheric Measurement Techniques*, 4, 1361–1381. <https://doi.org/10.5194/amt-4-1361-2011>
- Lawson, R. P., Baker, B. A., Pilon, B., & Mo, Q. (2006). In situ observations of the microphysical properties of wave, cirrus and anvil clouds. Part II: Cirrus clouds. *Journal of the Atmospheric Sciences*, 63, 3186–3203.
- Lawson, R. P., Pilon, B., Baker, B. A., Mo, Q., Jensen, E. J., Pfister, L., & Bui, P. (2008). Aircraft measurements of microphysical properties of subvisible cirrus clouds in the tropical tropopause layer. *Atmospheric Chemistry and Physics*, 8, 1609–1620.
- Lienhard, D. M., Huisman, A. J., Krieger, U. K., Rudich, Y., Marcolli, C., Luo, B. P., et al. (2015). Viscous organic aerosol particles in the upper troposphere: diffusivity-controlled water uptake and ice nucleation? *Atmospheric Chemistry and Physics*, 15, 13,599–13,613.
- Lin, R.-F., Starr, D. O., Reichardt, J., & DeMott, P. J. (2005). Nucleation in synoptically forced cirrus. *Journal of Geophysical Research*, 110, D08208. <https://doi.org/10.1029/2004JD005362>
- Lohmann, U., & Gasparini, B. (2017). A cirrus cloud climate dial? *Science*, 357, 248–249.
- Lohmann, U., Kärcher, B., & Hendricks, J. (2004). Sensitivity studies of cirrus clouds formed by heterogeneous freezing in the ECHAM GCM. *Journal of Geophysical Research*, 109, D16204. <https://doi.org/10.1029/2003JD004443>
- McFarquhar, G. M., Um, J., Freer, M., Baumgardner, D., Kok, G. L., & Mace, G. (2007). The importance of small ice crystals to cirrus properties: Observations from the tropical warm pool international cloud experiment (TWP-ICE). *Geophysical Research Letters*, 57, L13803. <https://doi.org/10.1029/2007GL029865>
- Mitchell, D. L., & Finnegan, W. (2009). Modification of cirrus clouds to reduce global warming. *Environmental Research Letters*, 4. <https://doi.org/10.1029/2007GL029865>
- Möhler, O., Benz, S., Saathoff, H., Schnaiter, M., Wagner, R., Schneider, J., et al. (2008). The effect of organic coating on the heterogeneous ice nucleation efficiency of mineral dust aerosols. *Environmental Research Letters*, 3, 025007. <https://doi.org/10.1088/1748-9326/3/2/025007>
- Murphy, D. M. (2014). Rare temperature histories and cirrus ice number density in a parcel and one-dimensional model. *Atmospheric Chemistry and Physics*, 14, 13,013–13,022. <https://doi.org/10.5194/acp-14-13013-2014>
- Murray, B. J. (2008). Inhibition of ice crystallisation in highly viscous aqueous organic acid droplets. *Atmospheric Chemistry and Physics*, 8, 5423–5433.
- Murray, B. J., Wilson, T. W., Dobbie, S., Cui, Z., Al-Jumr, S. M. R. K., Möhler, O., et al. (2010). Heterogeneous nucleation of ice particles on glassy aerosols under cirrus conditions. *Nature Geoscience*, 3, 233–237.
- Neff, J. C., Ballantyne, A. P., Farmer, G. L., Mahowald, N. M., Conroy, J. L., Landry, C. C., et al. (2008). Increasing eolian dust deposition in the western United States linked to human activity. *Nature Geoscience*, 1, 189–195. <https://doi.org/10.1038/ngeo133>
- Penner, J. E., Zhou, C., & Liu, X. (2015). Can cirrus cloud seeding be used for geoengineering? *Geophysical Research Letters*, 42, 8775–8782. <https://doi.org/10.1002/2015GL065992>
- Podglajen, A., Hertzog, A., Plougonven, R., & Legras, B. (2016). Lagrangian temperature and vertical velocity fluctuations due to gravity waves in the lower stratosphere. *Geophysical Research Letters*, 43, 3543–3553. <https://doi.org/10.1002/2016GL068148>
- Prenni, A. J., Petters, M. D., Faulhaber, A., Carrico, C. M., Ziemann, P. J., Kreidenweis, S. M., & DeMott, P. J. (2009). Heterogeneous ice nucleation measurements of secondary organic aerosol generated from ozonolysis of alkenes. *Geophysical Research Letters*, 36, L06808. <https://doi.org/10.1029/2008GL036957>
- Price, H. C., Mattsson, J., Zhang, Y., Bertram, A. K., Davies, J. F., Grayson, J. W., et al. (2015). Water diffusion in atmospherically relevant α -pinene secondary organic material. *Chemical Science*, 6, 4876–4883. <https://doi.org/10.1039/c5sc00685f>
- Schill, G. P., Haan, D. O. D., & Tolbert, M. A. (2014). Heterogeneous ice nucleation on simulated secondary organic aerosol. *Environmental Science & Technology*, 48, 1675–1682.
- Schill, G. P., & Tolbert, M. A. (2013). Heterogeneous ice nucleation on phase-separated organic-sulfate particles: Effect of liquid vs. glassy coatings. *Atmospheric Chemistry and Physics*, 13, 4681–4695.
- Schoeberl, M. R., Jensen, E. J., Podglajen, A., Coy, L., Lodha, C., Candido, S., & Carver, R. (2017). Gravity wave spectra in the lower stratosphere diagnosed from project loon balloon trajectories. *Journal of Geophysical Research: Atmospheres*, 122, 8517–8524. <https://doi.org/10.1002/2017JD026471>
- Sherwood, S. C., Chae, J.-H., Minnis, P., & McGill, M. (2004). Underestimation of deep convective cloud tops by thermal imagery. *Geophysical Research Letters*, 31, L11102. <https://doi.org/10.1029/2004GL019699>
- Solomon, S., Rosenlof, K., Portmann, R., Daniel, J., Davis, S., Sanford, T., & Plattner, G.-K. (2010). Contributions of stratospheric water vapor changes to decadal variations in the rate of global warming. *Science*, 327, 1219–1223.
- Spichtinger, P., Cziczo, D. J., & D14208 (2010). Impact of heterogeneous ice nuclei on homogeneous freezing events in cirrus clouds. *Journal of Geophysical Research*, 115. <https://doi.org/10.1029/2009JD012168>
- Spichtinger, P., & Krämer, M. (2013). Tropical tropopause ice clouds: A dynamic approach to the mystery of low crystal numbers. *Atmospheric Chemistry and Physics*, 13, 9801–9818.
- Storøy, T., Kristjánsson, J. E., Muri, H., Pfeffer, M., Barahona, D., & Nenes, A. (2013). Cirrus cloud seeding has potential to cool climate. *Geophysical Research Letters*, 40, 178–182. <https://doi.org/10.1029/2012GL054201>
- Thornberry, T. D., Rollins, A. W., Avery, M. A., Woods, S., Lawson, R. P., Bui, T. V., & Gao, R. S. (2017). Ice water content-extinction relationships and effective diameter for TTL cirrus derived from in situ measurements during ATTREX 2014. *Journal of Geophysical Research: Atmospheres*, 122, 4494–4507. <https://doi.org/10.1002/2016JD025948>

- Thornberry, T. D., Rollins, A. W., Gao, R. S., Watts, L. A., Ciciora, S. J., McLaughlin, R. J., & Fahey, D. W. (2015). A two-channel, tunable diode laser-based hygrometer for measurement of water vapor and cirrus cloud ice water content in the upper troposphere and lower stratosphere. *Atmospheric Measurement Techniques*, *8*, 211–244.
- Ueyama, R., Jensen, E. J., Pfister, L., & Kim, J.-E. (2015). Dynamical, convective, and microphysical control on wintertime distributions of water vapor and clouds in the tropical tropopause layer. *Journal of Geophysical Research: Atmospheres*, *120*, 10,483–10,500. <https://doi.org/10.1002/2015JD023318>
- Ueyama, R., Pfister, L., Jensen, E. J., Diskin, G. S., Bui, T. P., & Dean-Day J. M. (2014). Dehydration in the tropical tropopause layer: A case study for model evaluation using aircraft observations. *Journal of Geophysical Research: Atmospheres*, *119*, 5299–5316. <https://doi.org/10.1002/2013JD021381>
- Ullrich, R., Hoose, C., Möhler, O., Niemand, M., Wagner, R., Höhler, K., et al. (2017). A new ice nucleation active site parameterization for desert dust and soot. *Journal of the Atmospheric Sciences*, *74*, 699–717.
- Wagner, R., Höhler, K., Huang, W., Kiselev, A., Möhler, O., Mohr, C., et al. (2017). Heterogeneous ice nucleation of α -pinene SOA particles before and after ice cloud processing. *Journal of Geophysical Research: Atmospheres*, *122*, 4924–4943. <https://doi.org/10.1002/2016JD026401>
- Wagner, R., Möhler, O., Saathoff, H., Schnaiter, M., Skrotzki, J., Leisner, T., et al. (2012). Ice cloud processing of ultra-viscous/glassy aerosol particles leads to enhanced ice nucleation ability. *Atmospheric Chemistry and Physics*, *12*, 8589–8610.
- Wang, B. B., Lambe, A. T., Massoli, P., Davidovits, T. B. O. P., Worsnop, D. R., & Kmpof, D. A. (2012). The deposition ice nucleation and immersion freezing potential of amorphous secondary organic aerosol: Pathways for ice and mixed-phase cloud formation. *Geophysical Research Letters*, *117*, D16209. <https://doi.org/10.1029/2012JD018063>
- Wang, P.-H., Minnis, P., McCormick, M. P., Kent, G. S., & Skeens, K. M. (1996). A 6-year climatology of cloud occurrence frequency from stratospheric aerosol and gas experiment II observations (1985–1990). *Journal of Geophysical Research*, *101*, 29,407–29,429.
- Weigel, W., Borrmann, S., Kazil, J., Minikin, A., Stohl, A., Wilson, J. C., et al. (2011). In situ observations of new particle formation in the tropical upper troposphere: The role of clouds and the nucleation mechanism. *Atmospheric Chemistry and Physics*, *11*, 9983–10,010.
- Wilson, T. W., Murray, B. J., Wagner, R., Möhler, O., Saathoff, H., Schnaiter, M., et al. (2012). Glassy aerosols with a range of compositions nucleate ice heterogeneously at cirrus temperatures. *Atmospheric Chemistry and Physics*, *12*, 8611–8632.
- Wise, M. E., Baustian, K. J., & Tolbert, M. A. (2009). Laboratory studies of ice formation pathways from ammonium sulfate particles. *Atmospheric Chemistry and Physics*, *9*, 1639–1646.
- Woods, S., Lawson, R. P. R. P., Jensen, E. J., Bui, P., Thornberry, T., Rollins, A., et al. (2018). Microphysical properties of tropical tropopause layer (TTL) cirrus. *Journal of Geophysical Research: Atmospheres*, *123*, 6053–6069. <https://doi.org/10.1029/2017JD028068>
- Yang, Q., Fu, Q., & Hu, Y. (2010). Radiative impacts of clouds in the tropical tropopause layer. *Journal of Geophysical Research*, *115*, D00H12. <https://doi.org/10.1029/2009JD012393>
- Zobrist, B., Marcolli, C., Pedernera, D. A., & Koop, T. (2008). Do atmospheric aerosols form glasses? *Atmospheric Chemistry and Physics*, *8*, 5221–5244.
- Zobrist, B., Marcolli, C., Peter, T., & Koop, T. (2008). Heterogeneous ice nucleation in aqueous solutions: The role of water activity. *The Journal of Physical Chemistry*, *112*, 3965–3975.